Temporal Seismic Observation and Preliminary Hypocenter Determination of Aftershocks of the 2003 Bam Earthquake, Southeastern Iran

Sadaomi Suzuki[1]*, Sayyed Mahmoud Fatemi Aghda[2], Takeshi Nakamura[1], Takeshi Matsushima[3], Yoshihiro Ito[4], Hossein Sadeghi[5], Mehdi Maleki[2], Arash Jafar Gandomi[1] and Sayyed Keivan Hosseini[1]

[1] Department of Earth and Planetary Sciences, Faculty of Sciences, Kyushu University, Fukuoka, Japan

[2] Natural Disaster Research Institute of Iran, Tehran, Iran

[3] Institute of Seismology and Volcanology, Faculty of Sciences, Kyushu University, Shimabara, Japan

[4] National Research Institute for Earth Science and Disaster Prevention, Tsukuba, Japan

[5] Earthquake Research Center, Department of Geology, Faculty of Sciences, Ferdowsi University of Iran, Mashhad, Iran

Abstract

We investigate the hypocenter distribution of aftershocks of the 26 December, 2003, Bam earthquake Mw 6.5 using a temporal seismic network installed for 1 month from 6 February, 2004. Preliminary hypocenters were determined using automatic phase-picking and calculating software. The epicenters are distributed linearly about 20 km in length parallel 3.5 km west of the Bam fault, and extend from the south of Bam city to the heavily damaged area of eastern Bam city including Arg-e-Bam. The hypocenters are distributed vertically or slightly leaning toward the east in the depth range from 0 km to 15 km. Using the hypocenter distribution we propose a schematic 3-D structure model of the source fault distinguished from the Bam fault. Eastern Bam city is located just above the northern part of the source fault and also on the rupture propagation direction from the asperity. It may be a major reason why eastern Bam city suffered the heaviest damage.

Key words : the 2003 Bam earthquake, seismic observation, aftershock, hypocenter, source fault

1. Introduction

The Bam earthquake occurred in southeastern Iran at 1: 56 (UTC, 5: 26 local time) on 26 December, 2003 (Fig. 1 (a)). USGS (http: //earthquake.usgs.gov/ recenteqsww/Quakes/uscvad.htm) reported its hypocenter at 29.004°N, 58.337°E, depth 10 km and Mw is 6.6. *IIEES* (2004) also reported its epicenter located at 29.08°N, 58.38°E, depth 13.2 km. Teleseismic focal mechanisms from various groups [USGS; Yamanaka (2003); Yagi (2003)] show a steeply dipping, right lateral strike-slip fault. This earthquake caused catastrophic damage to Bam city and neighborhood villages with a total population of about 142,000. This earthquake killed about 31,800 persons [Asahishimbun newspaper, 2004] and injured tens of thousands. About 22% of the population in and around Bam city were killed. The well-known historic castle of Arg-e-Bam, the biggest adobe (mud brick) complex in the world, at about 2000 years old, was also severely damaged by the Bam earthquake.

The main reason for such major damage may be weak adobe and brick houses. However, the damage was unexpectedly great for the magnitude. This was our first motivation for performing the study. The

---

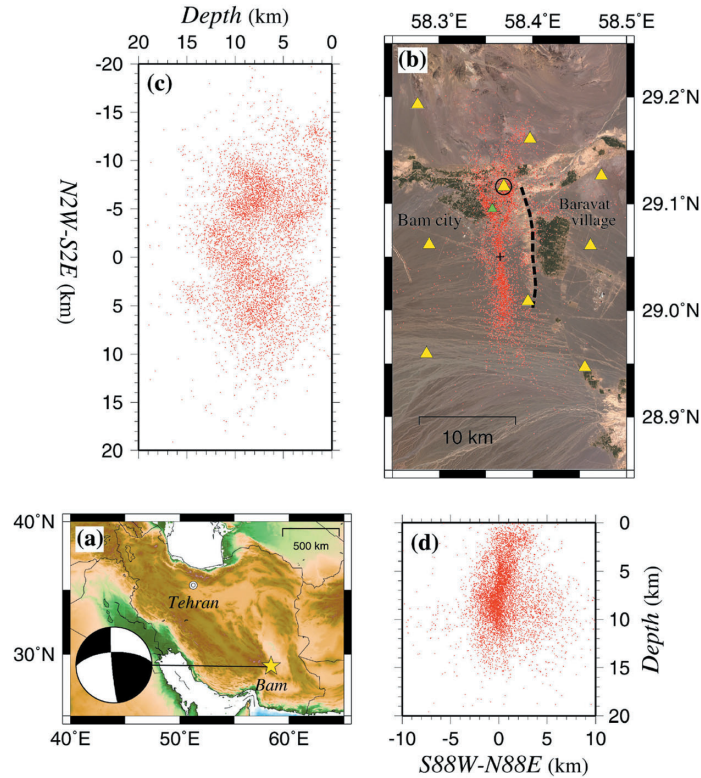＊present address: Tono Research Institute of Earthquake Science, Mizunami, 509-6132 Japan. (suzuki@tries.jp)

Fig. 1. Location map of Bam area and distribution of aftershock hypocenters of the 2003 Bam earthquake determined by automatic phase picking and calculation. (a) Location of the Bam earthquake in Iran. Focal mechanism of the mainshock (Yamanaka, 2003) is also shown. (b) Epicenter distribution (red dots) of aftershocks on the satellite map provided by NASA. Yellow triangles indicate the stations of the temporal seismic network we installed. The station in Arg-e-Bam is also marked by a circle. A small green triangle shows Bam station, which had a BHRC strong-motion accelerometer. A black dashed line indicates the traced line of the Bam fault referring to the geological map by *NGDI* (2003). (c) The cross-section projected in the N2°W-S2°E direction, parallel to the source fault. (d) The cross-section projected in the S88°W-N88°E direction, perpendicular to the source fault.

Bam fault, which was well known before the earthquake, is located along the west side of Baravat village, about 5 km southeast of Bam city. Just after the earthquake it was considered that the mainshock had occurred on the Bam fault [e.g., Shakib and Ahmadizadeh, 2004]. However, evidence of dislocation on this fault could not be found. Identifying the exact source fault of this earthquake was our second motivation. Moreover, the area with the heaviest damage is not Baravat village, which is close to the Bam fault, but the eastern half of Bam city 2–4 km from it. Knowing why Bam city suffered the worst damage was our third motivation. We, therefore, went to the Bam area for the seismological investigation, taking seismometers from Japan, and successfully observed more than 18,000 aftershocks using a temporal seismic network. In this paper we report on aftershock observations and preliminary results of
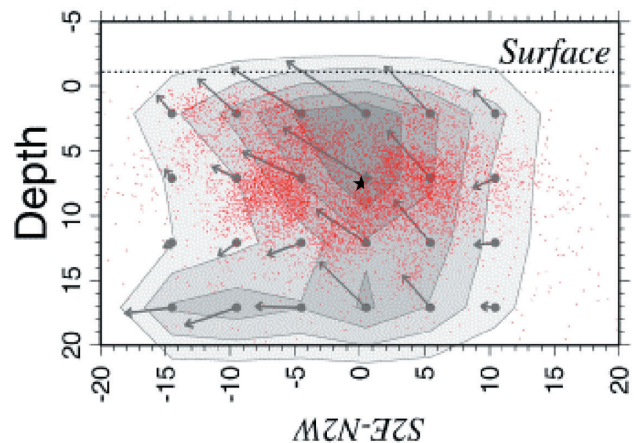

Fig. 3. Overlaying the hypocenter distribution (Fig. 1 c) upon the slip distribution (Yamanaka, 2004). Star shows the initial point of large slip movement (IPLSM).
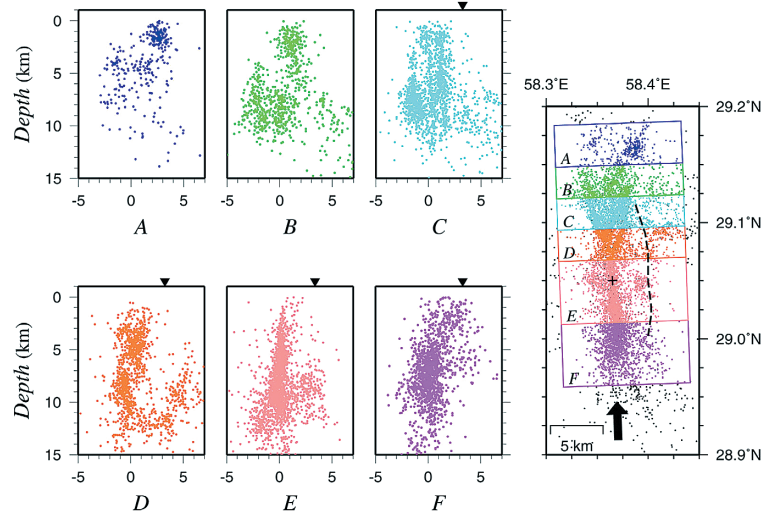
Fig. 4.   Detailed cross-sections of the aftershock distribution projected in the S88°W-N88°E direction.
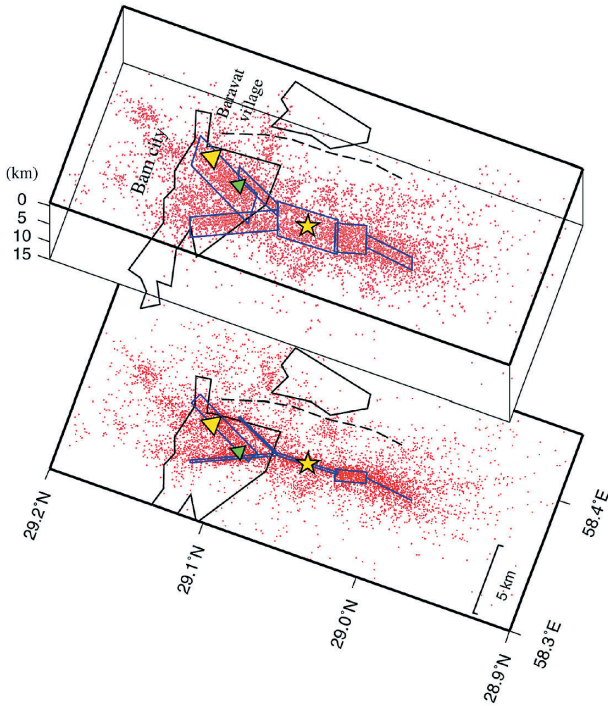

Fig. 5.   Schematic 3-D model of the source fault (blue rectangle) distinguished from the Bam fault (dashed line).   Yellow and green triangles show the locations of the Arg-e-Bam and Bam accelerograph station of BHRC, respectively.   A star indicates the initial point of large slip movement (IPLSM) of the mainshock inferred from the asperity area.
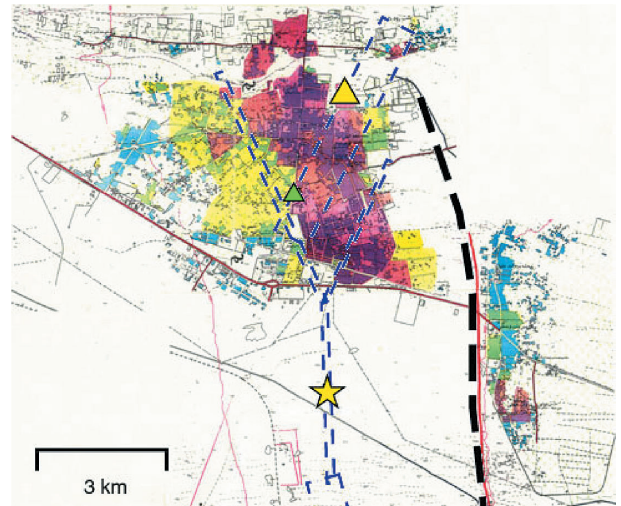

Fig. 6.   A map of the damaged area in and around Bam city [GSI, 2004].   Purple, red, and yellow correspond to 80–100%, 50–80%, and 20–50% damage rates.   Blue dashed lines present projected sections of the schematic source fault as shown in Fig. 5.   Triangles and star have the same meanings as those in Fig. 5.   The Bam fault is shown by a black dashed line.

data analysis.

2.   Aftershock Observation

A seismic network consisting of 9 temporal stations (Fig. 1 (b)) was installed in and around Bam city on 6 February 2004, about 6 weeks after the mainshock, and operation continued until 7 March 2004 (Table 1 and Photo 1).   The surface geology of the stations is shown in Table 2.   Geological site conditions at Stations 1, 4, 5, and 8 are very good.   Stations 2, 3, 6, 7, and 9 installed on alluviums containing pebbles are better for seismic observations than soil.   Each station was equipped with a 3-component high-sensitive seismograph (LE-3D, Lennartz Electronic)
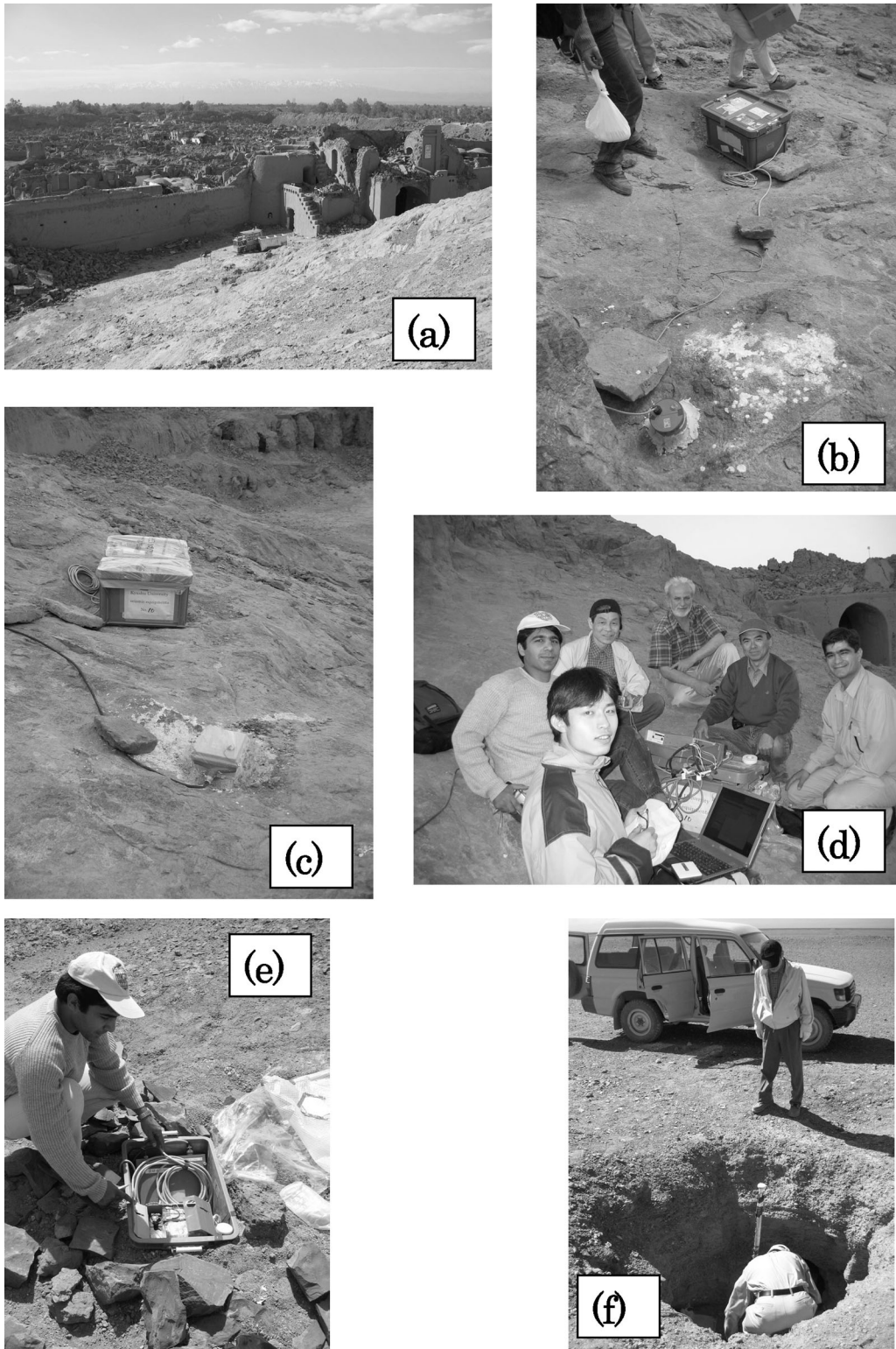
Photo 1. Example of temporal seismic stations and their instruments. (a) Station-5 in Arg-e-Bam. (b) High-sensitivity seismograph and its recording system of Station-5A installed on bedrock in Arg-e-Bam. (c) Strong motion accelerometer and its recording system of Station-5B installed on bedrock in Arg-e-Bam. (d) Member of seismic observation and manager of Arg-e-Bam (center). (e) Recording system of Station-8 on volcano-clastic andesite. The white circle in the right corner of the green box is the GPS antenna. (f) Installing GPS antenna on the top of a pole of Station-6 in the ruins of Qanat (Ghanat).

Table 1.　Seismic stations

Station	Station-0	Station-1	Station-2	Station-3	Station-4	Station-5A
Palace	Azad Hotel	15 km NW of Bam	5 km SW of Bam	15 km SW of Bam	8 km NNE of Bam	Arg-e Bam
Latitude(N, degree)	29.0899	29.1929	29.0615	28.9592	29.1607	29.116
Longitude(E, degree)	58.327	58.2771	58.2893	58.2864	58.3969	58.369
Altitude(m)	1049	1280	1202	1235	1080	1070
Seismograph	LenartzLE-3D	LenartzLE-3D	LenartzLE-3D	LenartzLE-3D	LenartzLE-3D	LenartzLE-3D
Start of Observation	Feb.5, evening	Feb.7,9:52	Feb.6,14:40	Feb.6,16:20	Feb.6,11:40	Feb.6,10:00
End of Observation	Feb.7	Mar.4, 01:51	Mar.6,16.20	Mar.6,16.50	Mar.6,06.20ut	Mar.5,17:50
Comment	Test of Observation	cable cut by animal	Problem of horizontal comp.	no problem	no problem	no problem

Station	Station-5B	Station-6	Station-7	Station-8	Station-9
Palace	Arg-e Bam	N of Railway	S of Airport	N of Airport	Medica Center
Latitude(N, degree)	29.116	29.0084	29.0607	29.1261	28.9466
Longitude(E, degree)	58.369	58.3949	58.4614	58.4731	58.4556
Altitude(m)	1070	1015	952	1006	905
Seismograph	Akashi-Accel.	LenartzLE-3D	LenartzLE-3D	LenartzLE-3D	LenartzLE-3D
Start of Observation	Feb.7,	Feb.6,16:20	Feb.7,15:07	Feb.6,about11:	Feb.6,17:40
End of Observation	Mar.5,17.50	Mar.7,10:20	Mar.7.09.20	Mar.6.12:20ut	Mar.7,10.50ut
Comment	problem of EW comp.	NS direction of sensor was reverse	no problem	no problem	GPS anttena fell horizontallly

Table 2.　Surface geology of Stations

Station No.	Description
1	Well-bedded ash fellow tuffs
2, 3, 6, 7, & 9	The area is covered with young sediments (Quaternary), and can be divided to the sandstone and micro-conglomerate at the bottom and alluviums on the top. The alluviums mostly contain of pebbles, gravel, and grains. The sites were installed on the alluviums. See Photo 1(f).
4	Well-bedded ash flow tuffs. This site was installed on some red marn and tuffs.
5	Bedrock of volcanic rock (andesite). See Photo 1(a)-(d)
8	Volcano-clastic andesite and alluvium containing pebbles. See photo 1(e)

The above information is taken from the Geological Map of Bam (1993).

of the velocity-type with a natural frequency of 1 Hz. At Station-5B in Arg-e-Bam (yellow triangle with circle in Fig. 1 (b)), we also installed a 3-component strong motion accelerometer (JEP-6A3, Akashi). The waveform data were continuously recorded at a sampling rate of 100 Hz by a data-logger (LS-8000SH, Hakusan) with 16 bit digits. The data-logger also has a GPS receiver for accurate time control. The seismic equipment was operated for about 1 month using 2 kinds of battery: 60 AH for a data-logger and 12 AH for a high-sensitive seismograph. Fig. 2 shows an example of aftershock waveforms recorded by the high-sensitive seismograph network. From this figure we can see clear onsets of P and S waves from

aftershocks. From this observation we obtained digitized data on more than 18,000 aftershocks.

3. Data Analysis

We scanned onsets of *P*- and *S*-waves automatically using the WIN software system [Urabe and Tsukada, 1991]. The hypocenter and the origin time were determined from these onset data using HYPOMH software [Hirata and Matsu'ura, 1987]. A velocity structure model from the 2002 Changoureh-Avaj earthquake (*M*w 6.5) in northwest of Iran [Suzuki *et al.*, 2003] was used for the hypocenter determination (Table 3). The *S*-wave velocity is assumed to be of $1/\sqrt{3}$ of the *P*-wave velocity. Hypocenters of the total number of 8123 aftershocks are determined automatically using arrival times of more than or equal to 5 stations. Their mean square residuals of *P*- arrival times are less than 0.44 sec. Average errors in those hypocenter locations are estimated to be 0.17, 0.14, and 0.34 km in the N-S, E-W, and depth directions, respectively.

4. Aftershock Distribution

Figure 1 (b) shows the epicenter distribution of aftershocks overlapping on a satellite image provided by NASA. Surprisingly, most of the epicenters are not on the geological Bam fault but are distributed in parallel about 3.5 km west [Suzuki *et al.,* 2004 a; Suzuki *et al.,* 2004 b]. The whole trend of the epicenter distribution is nearly linear in the direction of N 2°W-S 2°E. The dip angle of the hypocenter distri-

Table 3. Seismic velocity model for hypocenter determination

Depth (km)	Vp (km/s)
0.0	5.8
14.0	6.0
15.0	6.5
34.0	7.0
35.0	8.0

bution is nearly vertical or slightly leaning toward the east apparently on the S 88°W-N 88°E vertical cross-section (Fig. 1 (d)). The trends of epicenteral and hypocenteral distribution are in accord with the strike and dip angle of the focal mechanism (strike, dip, slip)=(175°, 85°, 153°) of the mainshock [Yamanaka, 2003] as shown in Fig. 1 (a). Horizontal length of the distribution is about 20 km with a depth range from 0 km to 15 km in the N 2°E-S 2°W vertical cross-section (Fig. 1 (c)). The source dimension is, therefore, roughly estimated to be 20 km×15 km. It is coincident with the results of Yamanaka (2003) and Yagi (2003), which are estimated from teleseismic data. This means that the hypocenter distribution of aftershocks occurring during the observation term presents a general view of the source fault structure of the Bam earthquake.

The distribution exhibits different features in the parts of south, middle, and north. In the southern part, most of the epicenters are aligned with a weak curve and are a little scattered. Its density is higher at depths of 5–10 km. In the middle part, epicenters are distributed as a thin line 5 km in length. In the cross-section (Fig. 1 (c)) a seismic gap can be distinguished at less than 8 km in depth. Das and Henry (2003) have generally suggested that few, and usually the smaller, aftershocks occur in high-slip regions of the fault. The seismic gap in Fig. 1 (c), therefore, may correspond to the higher slip region of 80 cm to 1 m proposed by Yamanaka (2003) as shown in Fig. 3. From this assumption we estimate that the initial point of large slip movement (IPLSM) of the mainshock is located at Lat.=29.050°N, Long.=58.365°E, Depth=7 km. We cannot suggest whether this initial point corresponds to the hypocenter (initial break point) or not from our own data. But, it may be considered that the relative distance between this initial point and the hypocenter is not so large. The northern part of the epicenter distribution shows dispersal. There is even a possibility of branches of the fault in the NNW and NNE directions. In this area some of the aftershocks occur at a shallower depth. We note that the northern part of the epicenter distribution corresponds to the populated area of Bam city. Arg-e-Bam is also located in the epicenter distribution (Fig. 1 (b)).
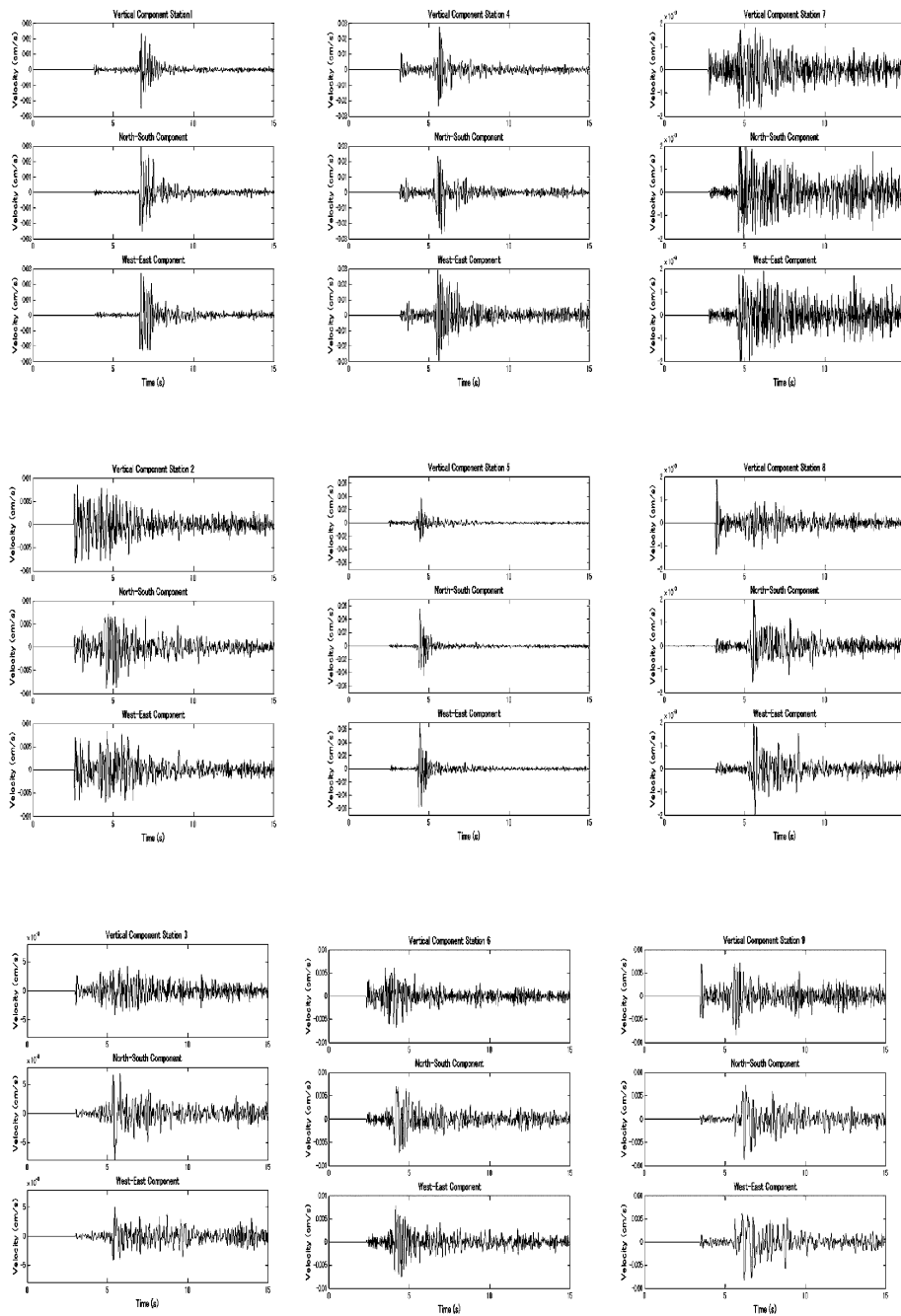
Fig. 2. An example of aftershock waveforms recorded by the high-sensitive seismograph network as shown in Fig. 1 (b). This aftershock occurred at Lat.: 29.0498, Long.: 58.3619, Depth: 11 km on February 20, 2004, 18: 54: 49, M: 2.8.

5. 3-D Structure of the Source Fault

Figure 4 shows detailed slices of the seismic cross-section in contrast with the location of the Bam fault on the ground (inverted triangle). In section E of the central region, the aftershock distribution clearly shows a direct vertical trend like a knife edge, not extending to the Bam fault. But, the trend in section F of the southern region is not clear but seems to be extending to the Bam fault. In sections of B, C, and D of the northern region the pattern of aftershocks is very complex with 3 main linear branches. Using more detailed slices of the hypocenter distribution we present a schematic model of the 3-D structure of the source fault in Fig. 5. The shape

of the fault in the central and southern region is rather simple, but seems to be slightly twisted. In the northern region there are 3 branching fault sections with different depth ranges. In this figure we also plot the locations of IPLSM (yellow star) estimated in the previous section, Arg-e-Bam (yellow triangle), and Bam accelerograph station (green triangle) of BHRC (Building and Housing Research Center), respectively.

6. Relation between Fault Structure and Damaged Area

Figure 6 shows a map of the damaged area in and around Bam city [GSI, 2004]. We also present a projection of the schematic structure of the source fault shown in Fig. 5 onto the damage map. Comparing the heavy damaged area with the projection of the source fault, considering the average errors of aftershock epicenters, we notice that most of the heavy damage, which is concentrated in the eastern region of Bam city, is located at or near the 3 fault parts in the northern part of the source fault. In this area, most of the houses (more than 80%) collapsed, and a very strong ground motion of 979.95 gals (vertical component) was recorded at the Bam accelerograph station of BHRC as shown by a green triangle in Figs. 5 and 6. This station is located near a branch point between the NNW part and NNE part of the fault. Its horizontal and 3-D distances from the assumed IPLSM of the mainshock are estimated to be about 5 km and 9 km, respectively. This 3-D distance is a little longer than 7 km estimated from S-P time of accelerogram at Bam station by BHRC (http://www.bhrc.gov.ir/Bhrc/d-stgrmo/shabakeh/earthquake/bam/bam.htm).

The area with the heaviest damage in eastern Bam city is located not only on the northern part of the source fault but also on the rupture propagation direction from the asperity. In general, strong seismic energy arrives due to directivity (e.g., Lay and Wallace, 1995). The relationship between the location of Bam city and rupture propagation direction must be one of the causes of the devastating damage. In contrast, Baravat village near the Bam fault was not as heavily damaged as eastern Bam city. Baravat village is located not on the source fault and not in the rupture propagation direction from the asperity. These spatial conditions may not give maximum damage to Baravat village.

7. Conclusion

We automatically determine the hypocenters of 8123 aftershocks of the December 26, 2003 Bam earthquake from February 6 through March 7, 2004 using a temporal seismic network. The distribution of aftershocks shows the following features.

1. The whole trend of the epicenter distribution is nearly linear about 20 km in length in the direction N 2°W-S 2°E, in parallel about 3.5 km west of the geological Bam fault on the ground.

2. The hypocenter distribution shows a trend of nearly vertical or slightly leaning to the east in a depth range from 0 km to 15 km. The whole trend is not oriented to the Bam fault.

3. Most of the heavy damage which was concentrated in the eastern region of Bam city including Arg-e-Bam is on the northern part of the source fault as inferred from aftershock distribution. We propose that this source fault is distinguished from the Bam fault.

4. By assuming correspondence between a seismic gap in the central part of the hypocenter distribution and the seismic asperity estimated from teleseismic data, the initial point of the large slip movement (IPLSM) of the mainshock is located at Lat.= 29.050°N, Long.=58.365°E, Depth=7 km.

5. The heavily damaged area in eastern Bam city is located not only on the source fault, but also in the rupture propagation direction from the asperity. It may be one of the main reasons why eastern Bam city suffered the heaviest damage.

Our aftershock results show the structure and the location of the source fault of the Bam earthquake, based on which we qualitatively propese why eastern Bam city suffered the heaviest damage. We need a more detailed quantitative study for evaluating the seismic hazards of the Bam earthquake as the next step.

References

Asahi-shimbun newspaper, December 25, 2004 (in Japanese).

Das, S. and C. Henry, 2003, Spatial relation between main earthquake slip and its aftershock distribution, *Rev. Geophysics,* **41**, 1013, doi: 10.1029/2002GR000119.

Geological map of Bam, 1993, 1:100000 series, sheet 7648-BAM, Geological survey of Iran.

GSI (Geological Survey of Iran), 2004, Bam earthquake of 26 December 2006, ICG reconnaissance mission, ICG report 2004-99-1, Report prepared for and in cooperation with Geological Survey of Iran, pp. 26.

Hirata, N. and M. Matsu'ura, 1987, Maximum-likelihood estimation of hypocenter with origin time eliminated using nonlinear inversion technique, *Phys. Earth Planet. Inter.,* **47**, 50-61.

IIEES (International Institute of Earthquake Engineering and Seismology), Earthquakes of 21th century, Data Bank, 2004. (Available at http://www.iiees.ac.ir/bank/bank¥_2003.html).

Lay, T. and T. Wallace, 1995, *Modern Global Seismology,* Academic Press, San Diego.

NGDI (National Geoscience Database of Iran), 2004, http://www.ngdir.ir/.

Shakib H. and M. Ahmadizadeh, 2004, On December 26, 2003 southeastern Iran Earthquake in Bam region, pp. 3,

Housing Foundation.

Suzuki, S., H. Sadeghi, S.K. Hosseini, Y. Fujii and S.M. Fatemi Aghda, 2003, Aftershock distribution and source parameters of the 22 June 2002 Changoureh earthquake (*M*w6.5), Northwest Iran, *IUGG Gen. Assem.* 2003, JSS 02/02A/D-002.

Suzuki, S., T. Matsushima, Y. Ito, T. Nakamura, S.K. Hosseini and N. Hirata, 2004 a, Preliminary report of strong motion and aftershock observation of the 2003/12/26 Bam earthquake (*M*w 6.5) in southeastern Iran, *Abstr. 2004 Jpn. Earth Planet. Sci. Joint Meeting,* S046-P001 (in Japanese with English abstract).

Suzuki, S., T. Matsushima, Y. Ito, S.K. Hosseini, T. Nakamura, A.J. Gandomi, H. Sadeghi, M. Maleki and F. Aghada, 2004 b, Source fault of the 2003/12/26 Bam earthquake (Mw 6.5) in southeastern Iran inferred from aftershock observation data by temporal high-sensitive-seismograph network, *Eos Trans. AGU,* **85** (17), Jt. Assem. Suppl., Abstract S23A-07.

Urabe, T. and S. Tsukada, 1991, A workstation-assisted processing system for waveform data from microearthquake networks, *Abstr. Spring Meeting of Seismological Society of Japan,* 70 (in Japanese).

Wessel, P. and W.H.F. Smith, 1991, Free software helps map and display data, *EOS Trans. Am. Geophys. Union,* **72**, 441.

Yagi, Y., 2003, Preliminary results of rupture process for 2003 December 26 southeastern IRAN, Earthquake, Source Process of Recent Large Earthquakes, International Institute of Seismology and Earthquake Engineering. (Available at http://iisee.kenken.go.jp/staff/yagi/eq/Iran20031226/IRAN20031226.htm).

Yamanaka, Y., 2003, Seismological Note: No.145, Earthquake Information Center, Earthquake Research Institute, University of Tokyo. (Available at http://wwweic.eri.u-tokyo.ac.jp/EIC/EUC¥_News/031226f.html).